Unusual Mechanism of Oxygen Atom Transfer and Product Rearrangement in the Catalytic Reaction of 2-Methyl-3-hydroxypyridine-5-carboxylic Acid Oxygenase†

Pimchai Chaiyen, Pierre Brissette, David P. Ballou,* and Vincent Massey

Department of Biological Chemistry, University of Michigan, Ann Arbor, Michigan 48109-0606

Received January 16, 1997; Revised Manuscript Received April 14, 1997⊗

ABSTRACT: The oxygenation reaction of 2-methyl-3-hydroxypyridine-5-carboxylic acid (MHPC) oxygenase with the substrate, MHPC, was investigated. Two oxygenated flavin intermediates C(4a)-hydroperoxy flavin and C(4a)-hydroxy flavin were found, implying that the enzyme functions similarly to flavoprotein hydroxylases. This finding is supported by the results of independent oxygen-18 tracer experiments, which showed that one atom of oxygen from $^{18}O_2$ and one atom of oxygen from $H_2{}^{18}O$ are incorporated in the product. MHPC oxygenase normally catalyzes both the oxygenation and the hydrolytic ring opening of the pyridine ring of MHPC to yield the acyclic compound, α-(*N*-acetylaminomethylene)succinic acid. Using 5-hydroxynicotinic acid (5HN), which has no 2-methyl group, we tested whether the hydrolytic reaction was due to the presence of the 2-methyl group on MHPC (that prevented rearomatization of the initial product) or to the specific properties of MHPC oxygenase. Product analysis of the enzymatic reaction of 5HN and MHPC oxygenase shows that the enzyme catalyzes the hydroxylation and subsequent hydrolysis of the hydroxylated substrate to yield an acyclic product. The investigation of the oxygenation reaction demonstrates that the enzyme uses the same mechanism to catalyze the 5HN reaction as it does in the MHPC reaction.

2-Methyl-3-hydroxypyridine-5-carboxylic acid (MHPC)[1] oxygenase (MHPCO) (EC 1.14.12.4) contains FAD and is involved in the degradation of vitamin B_6 (or pyridoxine) in bacteria (Sparrow et al., 1969). This enzyme is induced when bacteria are grown with pyridoxine or pyridoxamine as their sole source of carbon and nitrogen. The enzyme can be isolated as a pure flavoprotein from *Pseudomonas* MA-1 and was initially characterized by Snell and coworkers (Sparrow et al., 1969; Kishore & Snell, 1979, 1981a−c).

MHPCO incorporates two atoms of oxygen into its substrate with concomitant cleavage of the pyridine ring, as shown in eq 1. Previous oxygen-18 tracer experiments

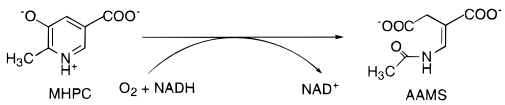

(1)

(Sparrow et al., 1969) were unable to establish whether both oxygen atoms derived from oxygen (dioxygenase) or whether one derived from solvent (monooxygenase). Nevertheless, MHPCO was classified as one of two known flavoprotein dioxygenases (Sparrow et al., 1969; Hayaishi et al., 1975). The details of the oxygenation mechanisms of these enzymes remain to be elucidated.

Structural and mechanistic studies on MHPCO indicated several similarities with flavin-containing monooxygenases (Sparrow et al., 1969; Kishore & Snell, 1979, 1981a−c). In its absolute requirement for enzyme-bound FAD and for reduced pyridine nucleotide electron donors for catalytic activity, MHPCO is closely related to the external flavoprotein monooxygenases (Massey & Hemmerich, 1975) and differs from the metalloprotein dioxygenases involved in the cleavage of homocyclic and heterocyclic aromatic compounds (Hayaishi et al., 1975; Nozaki, 1974). MHPCO also displays a steady state kinetic pattern consistent with a Bi Uni Uni Uni Ping-Pong mechanism (Sparrow et al., 1969; Kishore & Snell, 1981a), which resembles that for the aromatic flavoprotein hydroxylases (Ballou, 1982; Howell et al., 1972; Husain & Massey, 1979; Detmer & Massey, 1984; Powlowski et al., 1989a; Strickland & Massey, 1973; Wang & Tu, 1984). MHPCO is also similar to aromatic FAD-containing hydroxylases in that the substrate MHPC possesses an activating hydroxyl group *ortho* to the position of oxygenation. With all known aromatic flavoprotein hydroxylases, except for 3-hydroxybenzoate 6-hydroxylase (Wang et al., 1987), oxygen insertion occurs at a position *ortho* to the activating hydroxyl group (Massey & Hemmerich, 1975; Ballou, 1982, 1984). Flavoprotein hydroxylases activate oxygen by forming a C(4a)-FAD hydroperoxide (known as intermediate I) from the reaction of their reduced FAD cofactors with O_2. Intermediate I then hydroxylates the substrate to form a dienone (or dienimine) product, leaving a C(4a)-FAD hydroxide (known as intermediate III). Intermediate III then loses water to regenerate oxidized FAD (Massey & Hemmerich, 1975; Ballou, 1982, 1984; Entsch et al., 1976; Yorita & Massey, 1993).

MHPCO differs from aromatic flavoprotein hydroxylases in that the product of the reaction, AAMS, is an acyclic compound rather than an aromatic product. The methyl

† This work was supported by the U.S. Public Health Service, GM 20877 (D.P.B.) and GM 11106 (V.M.) and the Development and Promotion of Science and Technology Talent Project, Thailand (P.C.).

* To whom correspondence should be addressed.

⊗ Abstract published in *Advance ACS Abstracts,* June 15, 1997.

[1] Abbreviations: MHPC, 2-methyl-3-hydroxypyridine-5-carboxylic acid; MHPCO, 2-methyl-3-hydroxypyridine-5-carboxylic acid oxygenase; 5HN, 5-hydroxynicotinic acid; AAMS, α-(*N*-acetylaminomethylene)succinic acid; FAMS, α-(*N*-formylaminomethylene)succinic acid; E_{ox} and E_{red}, oxidized and reduced forms of MHPC oxygenase; DTT, dithiothreitol; E_I (intermediate I), C(4a)-hydroperoxy flavin enzyme; E_{III} (intermediate III), C(4a)-hydroxy flavin enzyme.

S0006-2960(97)00089-5 CCC: $14.00

group at the 2 position (oxygenation position) of MHPC, which distinguishes MHPC from aromatic flavoprotein hydroxylase substrates, prevents the rearomatization step that in other flavoprotein hydroxylases leads to the aromatic product from the initial dienone product. Therefore, to test whether the cleavage is a consequence of properties of the enzyme or of the substrate, we have also used 5-hydroxynicotinic acid (5HN), an MHPC analog without the methyl group at the 2 position; the product of 5HN can, in principle, rearomatize to form a catecholic product (or its tautomer). The identification of the products of the enzyme with MHPC and with 5HN might provide useful information for understanding the nature of the MHPCO reaction mechanism.

In this study, the oxygenation reactions of MHPCO with MHPC and with 5HN as substrates were investigated to characterize possible oxygenated flavin adducts and to compare them with those known for other flavoprotein hydroxylases. Oxygen-18 tracer experiments were carried out to establish whether the enzyme is a monooxygenase or a dioxygenase. The products of the reaction of MHPCO and 5HN were identified and show that the cleavage of the product ring is an intimate part of the mechanism of the enzyme rather than a consequence of the nature of the substrate.

MATERIALS AND METHODS

Reagents. NADH, NAD^+, glucose-6-phosphate, glucose-6-phosphate dehydrogenase, and sodium dithionite were from Sigma Chemical Company. Diazald (*N*-methyl-*N*-nitroso-*p*-toluenesulfonamide, 99%) and sodium azide were from Aldrich Chemical Company. ^{18}O-labeled oxygen gas ($^{18}O_2$, 97−98 atom % enrichment) and water ($H_2{}^{18}O$, 97−98 atom % enrichment) were from Cambridge Isotope Laboratories. Catalase (bovine liver) was from Calbiochem. 2-Methyl-3-hydroxypyridine-5-carboxylic acid (MHPC) and 5-hydroxynicotinic acid (5HN) were prepared as described previously (Chaiyen, et al., 1997). The concentrations of the following compounds were determined using known extinction coefficients at pH 7.0: NADH, $\epsilon_{340} = 6.22$ mM^{-1} cm^{-1} (Horecker & Kornberg, 1948); MHPC, $\epsilon_{326} = 4.4$ mM^{-1} cm^{-1} (Kishore & Snell, 1979). 5HN has an extinction coefficient of 4.19 mM^{-1} cm^{-1}(0.1 N NaOH) at 315 nm. MHPCO was purified as previously described by Chaiyen et al. (1997). The concentration of the purified enzyme was measured using the molar absorption coefficient per enzyme-bound FAD of 13 110 M^{-1} cm^{-1} at 454 nm (Kishore, 1981b).

Spectroscopic Studies. UV−visible absorbance spectra were recorded with a Hewlett-Packard diode array spectrophotometer (HP 8452A), a Cary model 219 double beam spectrophotometer, or a Cary 3E spectrophotometer. Single wavelength enzymatic assays were conducted with a Cary model 219 double beam spectrophotometer. All spectrophotometers were equipped with thermostated cell compartments. ^{1}H NMR spectra were recorded with a General Electric GN500, 500 MHz NMR instrument. Chemical shift values are reported in parts per million relative to tetramethyl silane.

Rapid Reaction Experiments. Rapid kinetics procedures followed those described in Chaiyen et al. (1997). Enzyme and substrate solutions were placed in glass tonometers fitted with cuvettes that permitted absorbance spectra to be recorded in preparation for stopped-flow experiments. Enzyme samples were made anaerobic by equilibration with oxygen-free argon as described (Chaiyen et al., 1997). Enzyme was anaerobically reduced with a solution of sodium dithionite delivered from a syringe attached to the tonometer. In studies of the oxidative half-reaction, a practical range of oxygen concentrations of 60−1000 μM could be achieved by equilibration of buffer solutions with certified nitrogen and oxygen gas mixtures (Matheson). Dissolved oxygen concentration in buffer solution was calculated according to equations derived in Hitchman (1978). The highest concentration of oxygen was obtained by equilibration of buffer solutions at 0 °C with 100% oxygen (1.9 mM).

Oxygen-18 Tracer Experiments. Enzyme reactions in the presence of $^{18}O_2$ and/or $H_2{}^{18}O$ were conducted in an apparatus identical to that described by Powlowski et al. (1987).

Reaction under Oxygen-18 Gas. Reactions were carried out in a spectrophotometric cuvette designed for anaerobic studies and similar to that described by Williams et al. (1979). A 3-way stopcock was used to connect the cuvette to an anaerobic gas train and to a breakseal flask containing $^{18}O_2$ (97−98 atom % enrichment). This arrangement permitted the contents of the cuvette to be made anaerobic prior to introduction of $^{18}O_2$. The cuvette contained 6.2 mM of MHPC, 3.9 μM of MHPCO (FAD content), 36 mM of glucose-6-phosphate, and 90 units of glucose-6-phosphate dehydrogenase in 2.1 mL of buffer. The side arm to the cuvette contained 0.5 μmol of NAD^+ in 20 μL of 5 mM Tris-sulfate buffer, pH 8.0.

The assembly was made anaerobic with 8−10 cycles of alternate evacuation and flushing with oxygen-free nitrogen. The cuvette was then left under a vacuum and $^{18}O_2$ gas was admitted by turning the 3-way stopcock to the breakseal flask. The cuvette was disconnected from the assembly after closing the stopcock on the cuvette. The enzymatic reaction was then initiated by adding the contents of the side arm to the reaction mixture. The progress of the reaction was followed spectrophotometrically at 25 °C by monitoring the consumption of MHPC in the 320−350 nm region. Spectra of the reaction mixture were recorded at timed intervals until changes in absorbance in the 320−350 nm region ceased. After completion (6−7 h), the reaction was quenched by the addition of 30 μL of 6 N HCl to bring the pH of the reaction mixture to 2.0.

Reaction in Oxygen-18 Water. Enzymatic reactions in $H_2{}^{18}O$ media were conducted in an assembly identical to that described above. The reaction mixture was prepared in 2.1 mL of buffer enriched with 36 atom % $H_2{}^{18}O$. The ^{18}O enrichment of the reaction mixture was determined after dilution of a commercial sample of $H_2{}^{18}O$ (97−98 atom % enrichment). The contents of the cuvette were thoroughly mixed and the reaction was initiated by addition of NAD^+ (or $NADP^+$) from the side arm. After completion of the reaction, samples were quenched with 30 μL of 6 N HCl.

Reaction with Oxygen-18 Gas and Water. This reaction was carried out in a medium enriched with 97 atom % $^{18}O_2$ and 92 atom % $H_2{}^{18}O$. The reaction medium was buffered with 50 mM sodium phosphate, pH 6.8. A 900 μL solution containing 13 μmol of MHPC and 75 μmol of glucose-6-phosphate in 50 mM sodium phosphate, pH 6.8 was lyophilized. The residue was resuspended in 900 μL of 97 atom % $H_2{}^{18}O$, and the solution was transferred to the main chamber of the cuvette. MHPCO (8.2 nmol) and glucose-

6-phosphate dehydrogenase (90 units) in a volume of 40 μL were added to the $H_2{}^{18}O$-enriched buffer solution. The side arm of the cuvette contained 0.5 μmol of NAD^+ in a volume of 10 μL. After the system was made anaerobic and $^{18}O_2$ gas (97 atom % enrichment) was introduced as above, the reaction was initiated by tipping in the contents of the side arm. Following completion of the reaction, the sample was not quenched with acid.

Product Isolation and Preparation for Mass Spectrometry. Proteins were removed from the samples by ultrafiltration in Centricon concentrators with YM-10 membranes. The filtrate was then transferred to a glass test tube and evaporated to dryness in a Speed Vac concentrator. The residue was triturated, and the product AAMS was extracted with several 2 mL portions of hot methanol. The combined methanol extracts (16 mL) were treated at 4 °C with an excess of ethereal diazomethane gas generated by the action of alkali on *N*-methyl-*N*-nitroso-*p*-toluenesulfonamide (Diazald) (Levitt, 1973). After 1 h, the excess diazomethane was destroyed by addition of dilute acetic acid in methanol. After evaporation of excess solvent, the resulting material was washed three times with 2 mL portions of ether. The washed material contained the derivatized product, dimethyl-α-(*N*-acetylaminomethylene) succinate (dimethyl-AAMS). The average quantity of dimethyl-AAMS recovered was 6.5 μmol, as calculated from the extinction coefficient of this compound at 266 nm [$\epsilon_{266nm} = 21\,700\ M^{-1}\ cm^{-1}$ in 0.1 N HCl (Sparrow et al., 1969)]. This represents an overall yield of 50%.

In preparation for mass spectrometry, the dimethyl ester of AAMS was purified using an ISCO liquid chromatograph (Lincoln, NE) equipped with a variable wavelength UV detector (ISCO). The sample was dissolved in 8 mL of 5% acetonitrile and filtered through an Acrodisc HPLC filter (pore size, 0.45 μm; Gelman Sciences). Aliquots of the filtered solution were analyzed using a Regis 5 μm ODS column (25 cm). Elution was performed isocratically with 20% acetonitrile at a flow rate of 0.5 mL/min and detection at 260 nm. The derivatized AAMS eluted with an average retention time of 13.3 min. Eluate fractions corresponding to the derivatized AAMS were combined and evaporated to dryness in a Speed Vac concentrator to give an off-white solid residue. Incorporation of ^{18}O-label into the derivatized product was analyzed by direct probe mass spectrometry. Electron-impact mass spectrograms were recorded at an ionization voltage of 25 eV.

Calculation of the Oxygen-18 Isotopic Enrichment of Dimethyl-AAMS. The isotopic enrichment of the product in ^{18}O label was calculated from the relative ion intensities at *m*/*z* 215 (M^+), 217 ($M^+ + 2$), and 219 ($M^+ + 4$). Incorporation of ^{18}O-label into the individual fragments *m*/*z* 173 and *m*/*z* 156 was determined from the relative ion intensities at *m*/*z* 173 and 175 and at *m*/*z* 156 and 158, respectively. The relative ion intensity at *m*/*z* 217, 219, 175, and 158 were corrected for the contributions arising from natural abundance isotope peaks.

Preparation of the Product of 5HN and MHPCO Reaction for NMR Spectroscopy. Preparation of the product of 5HN and MHPCO reaction for identification by NMR spectroscopy was carried out as follows. Enzyme (17 nmol), 5HN (13.2 μmol), and NADH (12 μmol) were mixed aerobically in 60 mL of 10 mM ammonium bicarbonate, pH 7.0, at 25 °C. The reaction was monitored at 340 nm to observe consumption of NADH, which occured in about 40 min. The enzyme was removed immediately after completion of the reaction by ultrafiltration with a Centriprep-30 concentrator. The filtrate was loaded onto a DEAE-Sepharose (fast flow) column (1.8 × 12 cm) prewashed with 200 mL of 1 M ammonium bicarbonate and then equilibrated in water. The column was washed with 80 mL of water and 400 mL of a gradient of 0−0.2 M ammonium bicarbonate. The elution was controlled at 2.5 mL/min by a flow rate and gradient controlling system built by Dr. Sandro Ghisla of the University of Konstanz, Germany. The eluate was monitored at 260 nm by an ISCO UA-5 detector.

NAD^+, the 5HN product, and 5HN were eluted at 15−30%, 45%, and 55% of the gradient, respectively. The fractions containing the 5HN product were pooled and freeze-dried until about 80% of the water was removed. The sample was thawed and evaporated in a rotary evaporator at 40 °C to dryness. Since the 5HN product was sensitive to air, this drying process was conducted in a manner that minimized the amount of air that contacted the sample. The rotary evaporator was flushed with nitrogen gas before removing the sample vessel, which was then capped. The sample was irrigated with dry nitrogen gas for 10 h to eliminate the remaining water. D_2O was then added to the sample and it was anaerobically transferred to an NMR tube previously flushed with argon.

RESULTS

Oxygen-18 Tracer Experiments. Enzymatic reactions in the presence of ^{18}O-labeled water and molecular oxygen and subsequent isolation and derivatization of the product AAMS were carried out as described under Materials and Methods. The extent of oxygen-18 incorporation into the enzymatic product was determined by electron-impact mass spectrometry. The mass spectrogram of natural abundance dimethyl-AAMS is shown in Figure 1A. This spectrogram shows a distinctive molecular ion peak at *m*/*z* 215 (M^+, 28% relative abundance) and the following daughter ions: 184 (M^+-OCH_3, 6%), 173 (M^+-$COCH_2$, 13%), 156 (M^+-$COOCH_3$, 43%), and 114 (M^+-$COCH_2$-$COOCH_3$, 100%). Fragmentation of the molecular ion *m*/*z* 215 to daughter ions was explained in terms of the reactions shown in Scheme 1.

The product AAMS, generated by the action of MHPCO in a reaction mixture that was 97% enriched in $^{18}O_2$, was isolated and analyzed by direct probe mass spectrometry after derivatization. The mass spectrogram of the methylated product is shown in Figure 1B. Comparison of this spectrum with that of unlabeled dimethyl-AAMS indicated the incorporation of ^{18}O from molecular oxygen. The mass spectrogram in Figure 1B showed a molecular ion peak at *m*/*z* 217 and daughter fragments at *m*/*z* 173 and 158.

The fractional incorporation of ^{18}O label into the derivatized product was calculated by using eq 2:

$$\frac{^{18}\text{O incorporated}}{\text{Dimethyl-AAMS}} = \frac{I_{217(cor)} + 2[I_{219(cor)}]}{I_{215} + I_{217(cor)} + 2[I_{219(cor)}]}\frac{1}{F} \quad (2)$$

where I_{215} = the relative ion intensity at *m*/*z* of 215, $I_{217(cor)/219(cor)}$ = the relative ion intensity at *m*/*z* of 217 and 219 corrected for the contribution arising from the natural abundance isotope peak, and F = fractional enrichment of oxygen-18 in the reaction medium.

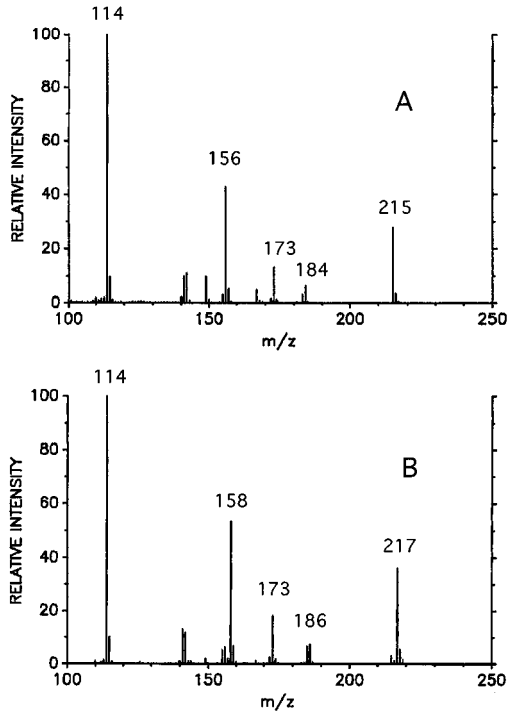

FIGURE 1: Mass spectrograms of natural abundance dimethyl-AAMS (A) and of dimethyl-AAMS isolated from a reaction mixture enriched with $^{18}O_2$ (B). (A) natural abundance AAMS was prepared enzymatically with MHPCO in a reaction mixture buffered with 50 mM sodium phosphate, pH 6.8. The isolated product was methylated and analyzed by direct probe mass spectrometry at an ionization voltage of 25 eV. (B) the product AAMS was prepared by the enzymatic action of MHPCO and MHPC in a reaction mixture enriched with $^{18}O_2$ (97 atom %) in 50 mM sodium phosphate, pH 6.8, at 25 °C. The mass spectrogram of the derivatized product was recorded at an ionization voltage of 25 eV.

Scheme 1

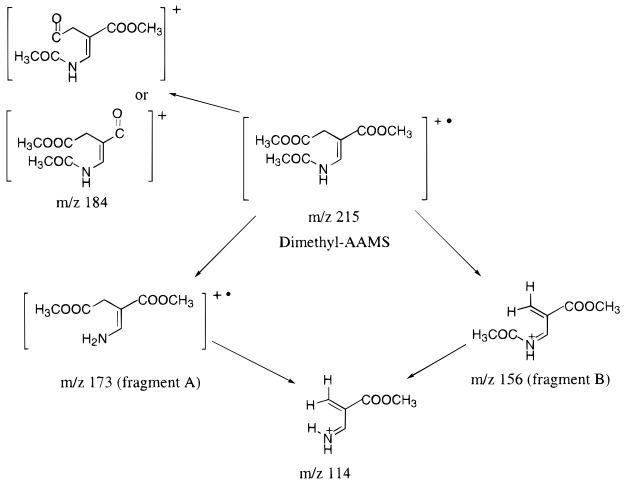

For the sample prepared under 97% enriched $^{18}O_2$ atmosphere, the observed relative intensity ratio of I_{215}:I_{217}:I_{219} is equal to 3.2:36.0:1.7 (see Figure 1B). The fractional incorporation of ^{18}O into product was then calculated to be 0.95. From the observed ion intensity ratios of I_{173}:I_{175} (18.4:0.6) and I_{156}:I_{158} (6.6:53.3) and using the same method of calculation as in eq 2, we calculated that fragment A and fragment B had incorporated 0.02 and 0.92 atom of oxygen-18, respectively.

Altogether, these results indicated that the product AAMS had incorporated 0.95 atom of ^{18}O. Analysis of the oxygen-18 content of the individual fragments demonstrated that the incorporated label was retained predominantly in fragment B (0.92 atom), reflecting incorporation of label into the newly formed acetyl moiety of the product AAMS. The small amount of incorporation of ^{18}O-label into fragment A (0.02 atom) indicates that minimal oxygen in the newly formed carboxyl group is derived from O_2.

Table 1: Incorporation of ^{18}O into the AAMS Product

	% ^{18}O incorporated into		
medium	AAMS	CH_3CO-	HO_2CCH_2-
$^{18}O_2$	0.95	0.92	0.02
$H_2{}^{18}O$	0.64	0.15	0.59
$^{18}O_2$ and $H_2{}^{18}O$	1.44	0.96	0.46

Complementary oxygen-18 tracer experiments were undertaken in reaction mixtures enriched with 36 atom % $H_2{}^{18}O$. Quantitative mass spectral analysis of the molecular ion region revealed that the derivatized product had incorporated 0.64 atom of ^{18}O. Analysis of the oxygen-18 content of fragments A and B indicated that 0.59 atom of ^{18}O was retained in fragment A (*m*/*z* 173). Fragment B (*m*/*z* 156) was found to contain 0.15 atom of ^{18}O label. The substantial incorporation of ^{18}O into fragment A from $H_2{}^{18}O$ reflects introduction of label into the newly formed carboxyl group of the product.

As a control experiment, the substrate MHPC was enzymatically converted to product in a buffered reaction medium enriched with 97 atom % $^{18}O_2$ and 92 atom % $H_2{}^{18}O$. Total incorporation of ^{18}O-label into the product AAMS was 1.44 atom, which was distributed as follows: 0.96 atom into the acetyl group and 0.46 atom in the carboxymethyl group.

Results from the oxygen-18 tracer experiments with MHPCO are summarized in Table 1.

Reoxidation of the Reduced Enzyme-MHPC Complex. Reduced enzyme−MHPC complex was mixed with oxygenated buffer in the stopped-flow spectrophotometer, and the reaction was monitored at 5−10 nm intervals between 350 and 500 nm; representative data recorded at 405 and 470 nm are shown in Figure 2 (solid lines). The return to oxidized enzyme consists of two phases. At 405 nm, a rapid increase in absorbance is followed by a smaller and slower decrease. The more rapid rate is dependent on oxygen concentration (inset of Figure 2) with a second-order rate constant of $5.5 \pm 0.2 \times 10^4$ M^{-1} s^{-1}, while the following phase is independent of oxygen concentration (0.86 ± 0.2 s^{-1}). At 470 nm, there is an initial lag period (corresponding to the rapid phase at 405 nm) followed by a large increase in absorbance at 0.86 ± 0.2 s^{-1}. This is consistent with formation of a flavin−oxygen intermediate that forms in a second-order reaction and decays to form oxidized enzyme. An absorbance spectrum of the intermediate was calculated (Figure 3) from data recorded at several wavelengths using 625 μM oxygen, and assuming a 2-step irreversible mechanism (Scheme 2) for the reoxidation ($k_1 = 34$ s^{-1}; $k_2 = 0.86$ s^{-1}). This spectrum has an absorption maximum at 385 nm ($\epsilon_{385} = 10\,200$ $M^{-1}cm^{-1}$) and is spectrally similar to flavin C(4a)-hydroperoxide adducts previously observed with all known flavin-dependent monooxygenases (Ballou, 1984; Palfey et al., 1996; Entsch et al. 1976; Powlowski et al., 1989a,b, 1990; Strickland & Massey, 1973; Schopfer & Massey, 1980; Detmer & Massey, 1985; Yorita & Massey, 1993; Arunachalam et al., 1994). This structural assignment

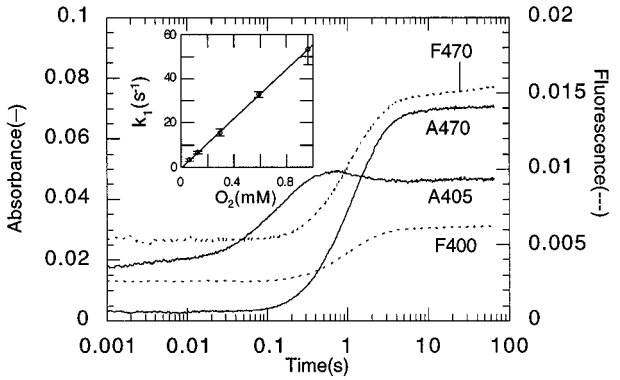

FIGURE 2: Reoxidation of reduced enzyme−MHPC complex. Reduced MHPCO (7 μM) was reacted with oxygen (130 μM) in buffer solution containing MHPC (344 μM) in the stopped-flow spectrophotometer. The reaction was followed by its absorbance at 405 nm (A405) and at 470 nm (A470). In a separate experiment, reduced MHPCO−MHPC complex [MHPCO (7.9 μM) and MHPC (300 μM)] were reacted with oxygen (130 μM) in buffer solution in the stopped-flow apparatus. The reaction was monitored by fluorescence with an excitation wavelength of 400 nm (F400), 470 nm (F470), and emission of wavelengths greater than 515 nm. All experiments were performed in 95 mM sodium phosphate buffer, pH 7.0, and 1 mM DTT at 4 °C. The inset figure shows the dependence of the observed rate constant for formation of the first intermediate on oxygen concentration.

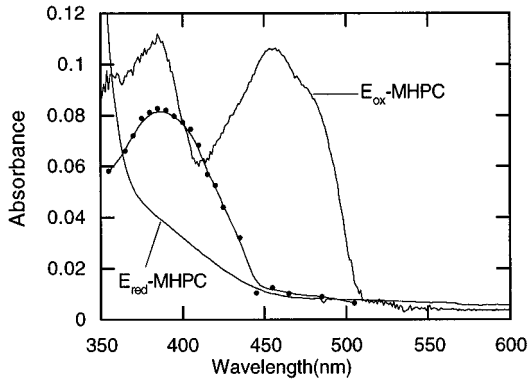

FIGURE 3: Calculated spectrum of the transient intermediate present during reoxidation of the reduced MHPCO−MHPC complex. Reduced MHPCO (8.1 μM) complexed with MHPC (300 μM) was reacted in the stopped-flow apparatus with buffer containing 625 μM oxygen. The reaction upon mixing was monitored at selected wavelengths ranging from 350 to 550 nm. The intermediate spectrum (filled circles) has a λ_{max} at 385 nm with an extinction coefficient of 10 200 M^{-1} cm^{-1}. For reference, the spectra of the reduced enzyme−MHPC complex (E_{red}−MHPC) and of the final enzyme species after reoxidation (E_{ox}−MHPC) are shown. The experiment was done in 95 mM sodium phosphate, pH 7.0, and 1 mM DTT at 4 °C.

Scheme 2: Reoxidation of the Reduced Enzyme−MHPC Complex[a]

$$E_{red}\text{–MHPC} + O_2 \xrightarrow{5.5 \pm 0.2 \times 10^4\ M^{-1}\ s^{-1}\ (A)} E_1\text{–MHPC} \xrightarrow[0.96 \pm 0.3\ s^{-1}\ (F)]{0.86 \pm 0.2\ s^{-1}\ (A)} E_{ox} + AAMS$$

[a] (A), (F) = rate constants determined by absorbance, and fluorescence methods. E_I = C(4a)-hydroperoxy-FAD enzyme.

is also supported by comparisons with data from flavin model compounds (Kemal & Bruice, 1976; Ghisla et al, 1977), and by ^{13}C NMR studies, which show that the flavin hydroperoxide intermediate in bacterial luciferase is a C(4a)-substitued flavin (Vervoort et al., 1986). The C(4a)-hydroperoxy flavin species is also referred to as intermediate I in accordance with the nomenclature of Entsch et al. (1976) for intermediates of *p*-hydroxybenzoate hydroxylase. Formation of the C(4a)-hydroperoxy flavin has been shown (Kemal & Bruice, 1976) to involve the transfer of a single electron from the reduced flavin singlet to triplet O_2 to avoid a spin-forbidden reaction. This flavin semiquinone and superoxide radical pair collapses to form the deprotonated C(4a)-peroxy flavin, which is then protonated to form C(4a)-hydroperoxy flavin.

The reoxidation of the reduced enzyme−MHPC complex was also studied in the same manner by fluorescence stopped-flow spectroscopy (Figure 2, dotted curves). Fluorescence excitation was at 400 nm and at 470 nm, and the fluorescence at wavelengths greater than 515 nm was observed. For both excitation wavelengths used, the reoxidation process results in a biphasic reaction with an initial lag process and a following phase of increasing fluorescence. The rate of the initial phase is dependent on oxygen concentration. This first phase of the fluorescence kinetic traces represents the formation of C(4a)-hydroperoxy-FAD enzyme and implies that this intermediate species has very little fluorescence. The rate of the second phase is 0.96 ± 0.3 s^{-1} and is not dependent on oxygen concentration. This second phase of the reaction represents the decay of the flavin hydroperoxide to form the oxidized enzyme species.

Scheme 2 describes the reoxidation of the E_{red}−MHPC complex as investigated by rapid kinetic techniques. In this reaction scheme, oxygen reacts with the reduced enzyme−MHPC complex to form the C(4a)-hydroperoxy-FAD enzyme (E_I−MHPC). Oxygen transfer from the transient intermediate to MHPC yields oxidized enzyme and the oxygenated product AAMS. In the presence of excess MHPC, the spectrum of the final enzyme species observed in the stopped-flow apparatus is that of the oxidized enzyme−MHPC complex.

Reoxidation of the Reduced Enzyme−MHPC Complex in Presence of Azide. It is known that for most flavoprotein hydroxylases, the presence of monovalent anions (such as azide) affects the rate constants of the oxygenation reaction so that the intermediates can be more fully distinguished. Although the mode of inhibition by azide is not completely understood, it has been observed with all flavoprotein hydroxylases that have been studied that the presence of azide results in clearer kinetic resolution of intermediates. It should be emphasized that the presence of azide primarily affects the kinetics of the overall reaction without changing the nature of intermediates and products. When we included 50 mM azide in the reaction mixture, the return to oxidized enzyme occurred with three phases (Figure 4). The first phase in the reoxidation process results in an increase in absorbance at 410 nm and a lag period at 470 nm. The rate of this phase is dependent on oxygen concentration (inset of Figure 4). This phase represents the generation of the first intermediate species with a second-order rate constant of 5.6 ± 0.1 × 10^4 M^{-1} s^{-1}, very similar to the oxygen reaction in the absence of azide. The second kinetic phase of the reoxidation is associated with a decrease in absorbance at 410 nm and an increase in absorbance at 470 nm with the rate of 1.0 ± 0.1 s^{-1}. This phase represents the conversion of the first transient intermediate to a second enzyme species. The third phase results in a large increase in absorbance at 470 nm and small increase in absorbance at 410 nm. This phase (0.35 ± 0.05 s^{-1}) represents the decay of the second

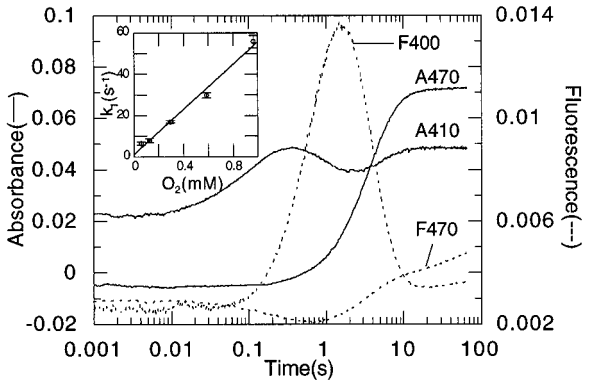

FIGURE 4: Reoxidation of reduced enzyme−MHPC complex in presence of azide. Reduced MHPCO (7 μM) was reacted with oxygen (130 μM) in buffer solution containing MHPC (344 μM) and 50 mM sodium azide in the stopped-flow spectrophotometer. The reaction was observed by its absorbance at 410 nm (A410) and 470 nm (A470). In a separate experiment, reduced MHPCO (7.9 μM) was reacted with oxygen (130 μM) in buffer solution containing 300 μM MHPC and 50 mM sodium azide in the stopped-flow apparatus. The reaction was monitored by fluorescence with excitation wavelength at 400 nm and emission of wavelengths greater than 408 nm (F400) and with excitation wavelength at 470 nm and emission of wavelength greater than 515 nm (F470). All experiments were performed in 95 mM sodium phosphate, pH 7.0, and 1 mM DTT at 4 °C. The inset figure shows the dependence of the observed rate constant of formation of the first intermediate on oxygen concentration.

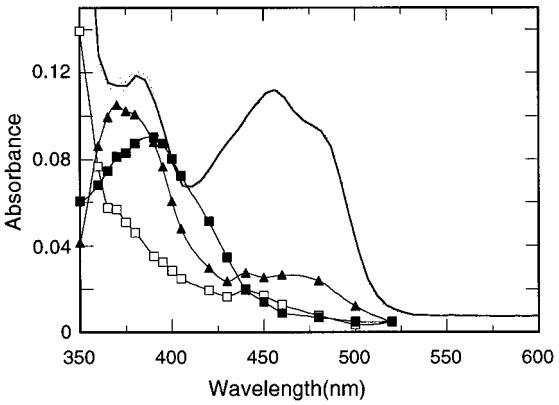

FIGURE 5: Spectra of the transient intermediates formed during reoxidation of the reduced MHPCO−MHPC complex in the presence of azide. The reaction of reduced MHPCO−MHPC complex (8.5 μM enzyme and 300 μM MHPC) with 625 μM oxygen in the presence of 50 mM sodium azide was monitored at several wavelengths in the stopped-flow apparatus. (□) Reduced enzyme−MHPC complex. (■) First intermediate. (▲) Second intermediate. (—) Oxidized enzyme. The experiment was done in 95 mM sodium phosphate, pH 7.0, 1 mM DTT, at 4 °C.

intermediate and is concomitant with the appearance of the oxidized enzyme.

The absolute absorbance spectra of the two transient enzyme intermediates can be calculated from knowledge of the apparent reaction rates associated with a suitable kinetic model of the reoxidation (Entsch et al., 1976; Schopfer & Massey, 1980). Intermediate spectra were calculated (Figure 5) on the basis of a sequential irreversible mechanism (A → B → C → D). The spectral properties of the intermediates are characteristic of C(4a)-substituted flavins with absorbance maxima in the 370−390 nm region (Kemal & Bruice, 1976; Ghisla et al., 1977). However, the calculated spectrum of the second intermediate showed considerable absorbance in the 450 to 500 nm region. It is known from studies of model compounds (Kemal & Bruice, 1976; Ghisla et al., 1977) and

Scheme 3: Reoxidation of the Reduced Enzyme−MHPC Complex in Presence of Azide[a]

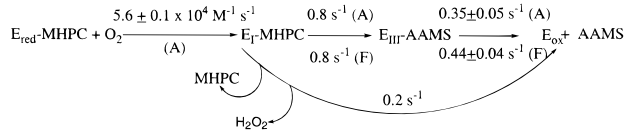

[a] E_I = C(4a)-hydroperoxy-FAD enzyme. E_{III} = C(4a)-hydroxy-FAD enzyme.

flavoprotein hydroxylases (Entsch et al., 1976; Entsch & Ballou, 1989; Schopfer & Massey, 1980; Detmer & Massey, 1985; Powlowski et al., 1989a,b, 1990) that C(4a)-substituted flavins, either free in solution or bound to enzymes, have minimal absorbance in the 450−500 nm region. The additional absorbance present in the spectrum of the second intermediate in the 450−500 nm region was assumed to arise from a bifurcation path in which the first intermediate decays partly to oxidized enzyme (*ca.* 20%) without formation of the second intermediate. Therefore, the observed rate constant of the second phase (1.0 ± 0.1 s^{-1}) is the summation of rate constants of the formation of E_{III}−AAMS step (*ca.* 0.8 s^{-1}) and the uncoupling step (*ca.* 0.2 s^{-1}) (Scheme 3).

The first intermediate had an absorbance maximum at 390 nm with an extinction coefficient of 10 060 M^{-1} cm^{-1}. Conversion to the second intermediate resulted in a shift of the absorbance maximum to shorter wavelengths. This intermediate absorbed maximally at 360 nm with an extinction coefficient of 11 800 M^{-1} cm^{-1}. It should be mentioned that calculated spectral properties of wavelengths shorter than 350 nm are less accurate due to the large background absorbance of MHPC in this region. We assigned the first and second intermediates as being the C(4a)-hydroperoxy flavin and C(4a)-hydroxy flavin enzymes, respectively. This assignment is based on observations that in flavin model compounds (Ball & Bruice, 1980; Kemal et al., 1977) and in flavin-dependent monooxygenases (Entsch et al., 1976; Entsch & Ballou, 1989; Schopfer & Massey, 1980; Detmer & Massey, 1985; Powlowski et al., 1990; Beaty & Ballou, 1981), the conversion of the C(4a)-hydroperoxy flavin to its C(4a)-hydroxy flavin derivative is accompanied by a similar small shift of the absorbance maximum in the near UV. The magnitude of this shift varies between 10 to 20 nm.

The results obtained from monitoring the reoxidation of the reduced enzyme−MHPC complex by stopped-flow fluorimetry are complementary to the absorbance data (Figure 4, dotted traces). The fluorescence excited at 400 nm results in a tetraphasic trace. The initial lag phase, which corresponds to the formation of C(4a)-hydroperoxy flavin, is dependent on oxygen concentration and the following phase with increasing fluorescence is associated with the formation of the highly fluorescent C(4a)-hydroxy flavin, which decays to the oxidized enzyme in the third phase. Excitation at 470 nm monitors the fluorescence of the oxidized enzyme species, and the reaction also shows four phases. At this wavelength, the formation of the C(4a)-hydroperoxy flavin and the C(4a)-hydroxy flavin both result in slightly decreased fluorescence. An increase in fluorescence is observed with the appearance of oxidized flavin. At both excitation wavelengths, there is also a slower fourth phase that is not observed in absorbance mode. This phase may be due to a slow dissociation of FAD from the enzyme, resulting in increased fluorescence.

Scheme 3 describes the reaction of oxygen with the E_{red}−MHPC complex in the presence of azide. In this reaction

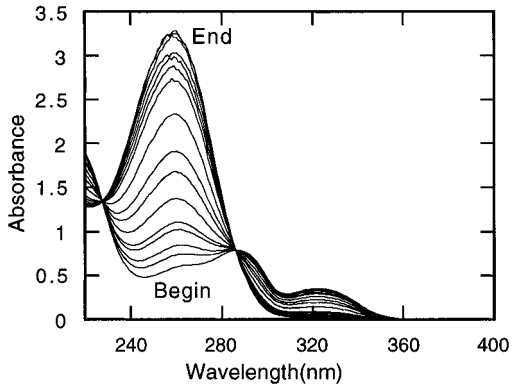

FIGURE 6: Conversion of 5HN to product by MHPCO. 5HN (255 μM) was reacted with NADH (generated continuously by including 5 μg/mL NAD^+, 1 mM glucose-6-phosphate, and 1 unit/mL of glucose-6-phosphate dehydrogenase in the reaction mixture) and MHPCO (75 nM) in air saturated 50 mM sodium phosphate, pH 7.0. The same reaction mixture without 5HN was put in the reference cell; thus, the spectra observed are those of 5HN and the enzymatic product spectrum. 5HN has λ_{max} at 288 and 323 nm as shown at the beginning of the reaction, and the 5HN product has a λ_{max} at 260 nm as shown at the end of the reaction (8 hr).

scheme, oxygen reacts with the reduced enzyme−MHPC complex to form the C(4a)-hydroperoxy-FAD enzyme (E_I). Oxygen transfer from E_I to MHPC yields the C(4a)-hydroxy-FAD enzyme (E_{III}) and the oxygenated product AAMS. The C(4a)-hydroxy-FAD enzyme then dehydrates to return to the oxidized enzyme species.

Identification of the Product of 5HN and MHPCO Reaction. We have studied the enzyme with 5HN, a substrate lacking the 2-methyl group, such that the initially formed dienone product could rearomatize. We have previously shown that the binding of 5HN to the enzyme stimulates the reductive half reaction of the enzyme in essentially the same way as does MHPC (Chaiyen et al., 1997), implying that 5HN binds properly. 5HN was converted to its product by a catalytic amount of enzyme and a small amount of NADH generated constantly by glucose-6-phosphate and glucose-6-phosphate dehydrogenase (Figure 6). The spectrum of the product derived from 5HN has an absorption maximum at 260 nm that is similar to that of AAMS, the enzymatic product of MHPC (Sparrow et al., 1969). This suggests that the product is not an hydroxypyridine, but is likely the ring-cleaved species.

The ^{1}H NMR spectrum of the product derived from 5HN (D_2O, d_6-DMSO) showed peaks at δ 3.25 (2H, s, $-CH_2-$), 7.73 (1H, s, $=CH-$), 8.28 ppm (1H, s, $-HCO$). ^{13}C NMR spectrum (decoupled) had peaks at δ 37.0, 120.5, 128.0, 163.0, 175.5, 179.0 ppm. From the ^{1}H and ^{13}C NMR data, the 5HN product was identified as α-(*N*-formylaminomethylene)succinic acid (A). The NMR spectrum of a similar

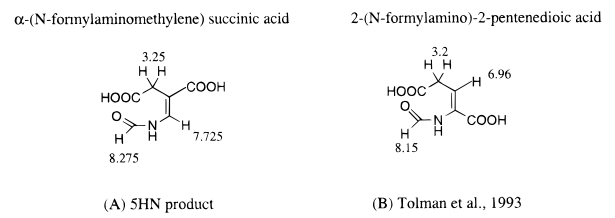

(A) 5HN product (B) Tolman et al., 1993

compound, 2-(*N*-formylamino)-2-pentenedioic acid (B) (Tolman et al., 1993), was reported to have similar chemical shifts to the 5HN product with the ^{1}H NMR spectrum having peaks at δ 3.20 (2H, d, $-CH_2-$), 6.96 (1H, t, $=CH-$), 8.15 ppm (1H, s, $-HCO$). The ^{13}C NMR spectrum had peaks at δ 34.0 (t), 125.8 (s), 129.4 (d), 159.8 (d), 165.2 (s), 172.0 ppm (s). The agreement of the NMR data of these two compounds implies that the 5HN product was indeed α-(*N*-formylaminomethylene)succinic acid.

5,6-Dihydroxynicotinic acid, the alternative rearomatized product of the reaction of 5HN and MHPCO, has been synthesized by Dallacker et al. (1979) and has been shown to have NMR signals of 7 and 7.57 ppm (one proton each signal), but none in the 3 ppm region. This again implies that the 5HN product is α-(*N*-formylaminomethylene)-succinic acid rather than 5,6-dihydroxynicotinic acid.

Hydroxylation Stoichiometry with 5HN as Substrate. The stoichiometry of the oxygenase-catalyzed reaction was determined by measuring with a Clark oxygen electrode and Yellow Springs oxygen monitor model 53, the amount of oxygen consumed and any H_2O_2 produced. The reaction mixture contained 193 μM NADH, 368 μM MHPC (or 411 μM 5HN), and 260 μM oxygen in 50 mM sodium phosphate buffer (1.5 mL), pH 8.0, at 25 °C. The reaction was started by addition of 2.6 nmol of MHPCO. The quantity of oxygen consumed was 193 μM, which was the same as the amount of NADH in the mixture. The small quantity of H_2O_2 that resulted was determined by adding catalase (2200 units) at the end of the reaction to convert one-half of the resultant H_2O_2 to O_2, and this was monitored with the oxygen electrode. The quantity of hydroxylated substrate was obtained by substracting the amount of H_2O_2 produced from the total oxygen consumed. The ratio of the hydroxylated product to oxygen consumed was 0.92 ± 0.01 for 5HN and 0.91 ± 0.01 for MHPC.

Reoxidation of Reduced Enzyme−5HN Complex. The reduced enzyme−5HN complex was mixed with oxygenated buffer in a diode array stopped-flow spectrophotometer, scanning from 350 to 650 nm. Global analysis using the model A → B → C → D solves for the spectra of two intermediates as shown in Figure 7. The first intermediate (2) has spectral characteristics of a C(4a)-hydroperoxy-FAD enzyme (see the above results of MHPC case). The rate of formation of this C(4a)-hydroperoxy-FAD is dependent on oxygen concentration (inset of Figure 7) and has a second-order rate constant of $(8.6 \pm 0.1) \times 10^4$ M^{-1} s^{-1}. The second intermediate (3) has spectral characteristics similar to those of the oxidized enzyme with high absorbance between 360 and 380 nm and in the 450 nm region, and the rate of formation of this intermediate is independent of O_2 concentration. This intermediate spectrum may be due to a mixture of oxidized enzyme and the C(4a)-hydroxy-FAD-5HN complex (intermediate III-5HN) as in Scheme 4. A similar C(4a)-hydroxy-FAD−substrate complex was observed with phenol hydroxylase in the presence of resorcinol as substrate (Yorita & Massey, 1993). The trapped C(4a)-hydroxy-FAD−5HN complex slowly decayed to the oxidized enzyme species as shown in the final spectrum. Note that the spectrum of the intermediate III−product complex was not detected, since its decay rate is much faster than its rate of formation (4.0 ± 0.5 s^{-1}). The reaction was also analyzed by single wavelength kinetics experiments at 380, 405, 443, and 470 nm as in the MHPC case. The rate constants obtained by single wavelength kinetics agreed very well with the values obtained by the global analysis method.

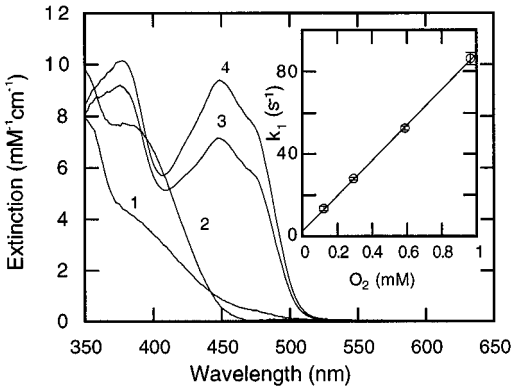

FIGURE 7: Reoxidation of the reduced enzyme−5HN complex. The reaction of reduced MHPCO−5HN complex (23 μM enzyme and 200 μM 5HN) with 625 μM oxygen was monitored in the diode array stopped-flow spectrophotometer. Global analysis shows the existence of four species involved in the reoxidation process: (1) the reduced enzyme−5HN complex; (2) intermediate I [the C(4a)-hydroperoxy-FAD] (note that the high absorbance below 370 nm region is due to the excess amount of 5HN); (3) the combination spectrum of the oxidized enzyme and intermediate III [the C(4a)-hydroxy-FAD]−5HN complex; (4) the oxidized enzyme−5HN spectrum. The inset figure shows the dependence of the observed rate constant for formation of the C(4a)-hydroperoxy-FAD enzyme on oxygen concentration. All experiments were done in 95 mM sodium phosphate, pH 7.0, and 1 mM DTT at 4 °C.

Scheme 4: Reoxidation of Reduced Enzyme−5HN Complex

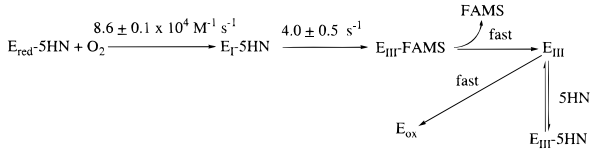

Scheme 4 describes the reoxidation of the E_{red}−5HN complex. In this reaction scheme, oxygen reacts with the reduced enzyme−5HN complex to form the C(4a)-hydroperoxy-FAD enzyme (E_I−5HN). Oxygen transfer from the transient intermediate to 5HN yields C(4a)-hydroxy-FAD (E_{III}−FAMS). A major fraction of this C(4a)-hydroxy-FAD enzyme rapidly releases H_2O to generate the oxidized enzyme, but some of the C(4a)-hydroxy-FAD enzyme forms a complex with the excess 5HN, resulting in the intermediate III−5HN complex.

Reoxidation of Reduced Enzyme−5HN Complex in Presence of Azide. The reduced enzyme−5HN complex was mixed with oxygenated buffer and 50 mM azide in the diode array spectrophotometer, scanning from 350 to 650 nm. Global analysis using the model A → B → C → D → E shows three intermediates (Figure 8). The first intermediate (2) has an absorption maximum at 392 nm and was assigned as intermediate I, the C(4a)-hydroperoxy-FAD enzyme (see the above results of MHPC case). The rate of formation of the first intermediate is dependent on oxygen concentration and has a rate constant of $(7.8 \pm 0.8) \times 10^4$ M^{-1}s^{-1} (Figure 8, inset). The second intermediate (3) has a λ_{max} at 356 nm as well as some absorbance in the 440−490 range. Thus, this step constitutes a bifurcation pathway with 85% of the enzyme forming intermediate III−FAMS [C(4a)-hydroxy-FAD−FAMS] (see the above result of MHPC case) with an observed rate constant of 4.3 ± 0.5 s^{-1} and 15% of the enzyme eliminating H_2O_2 to yield the oxidized enzyme species. Thus, rate constants for the formation of E_{III}−FAMS and the uncoupling pathway can be calculated to be 3.7 s^{-1} and 0.6 s^{-1}, respectively (Scheme 5). The third

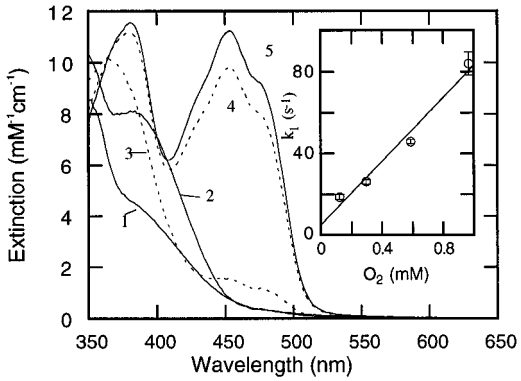

FIGURE 8: Reoxidation of the reduced enzyme−5HN complex in presence of azide. The reaction of reduced MHPCO−5HN complex (23 μM enzyme and 200 μM 5HN) with 625 μM oxygen in the presence of 50 mM sodium azide was monitored in the diode-array stopped-flow spectrophotometer. Global analysis shows the existence of five species involved in the reoxidation process: (1) the reduced enzyme−5HN complex; (2) intermediate I [the C(4a)-hydroperoxy-FAD] (note that the high absorbance below 370 nm region is partially due to the excess amount of 5HN); (3) intermediate III [the C(4a)-hydroxy-FAD], the absorbance in the 430−500 nm region is due to oxidized enzyme that arises from the uncoupling pathway; (4) the combination spectrum of the oxidized enzyme and the intermediate III−5HN complex; (5) the oxidized enzyme spectrum. The inset figure shows the dependence of the observed rate constant of formation of the C(4a)-hydroperoxy-FAD enzyme on oxygen concentration. All experiments were in 95 mM sodium phosphate, pH 7.0, 1 mM DTT at 4 °C.

Scheme 5: Reoxidation of Reduced Enzyme−5HN Complex in Presence of Azide

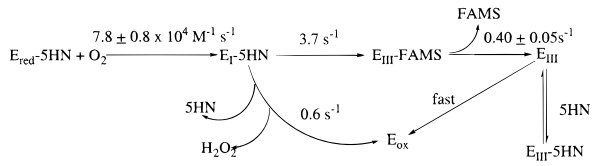

intermediate (4) has spectral characteristics of oxidized enzyme with high absorbance in the 360−380 region. This step is likely the formation of oxidized enzyme with some enzyme trapped as an intermediate III−5HN complex as shown in Scheme 5. This intermediate III complex slowly converts to the oxidized enzyme species.

The reoxidation of the reduced enzyme−5HN complex in the presence of azide was also investigated by the fluorescence stopped-flow method. Representative fluorescence kinetics traces can be compared to absorbance traces in Figure 9. With excitation at 400 nm for monitoring intermediate fluorescence and excitation at 470 nm for monitoring oxidized enzyme fluorescence, the fluorescence traces displayed four phases. The initial lag phase (excitation at 400 nm) and the initial fluorescence quenching phase (excitation at 470 nm) corresponded to the increase in absorbance at 410 nm associated with the formation of the C(4a)-hydroperoxy-FAD enzyme. The second phase results in increases of fluorescence at both excitation wavelengths. This step is the decay of the relatively unfluorescent C(4a)-hydroperoxy-FAD enzyme to a highly fluorescent C(4a)-hydroxy-FAD enzyme. During this step, some of the C(4a)-hydroperoxy-FAD enzyme converts directly to oxidized enzyme species without hydroxylation, as indicated by the small increase in absorbance at 470 nm and the small increase in fluorescence with excitation at 470 nm. The third phase is the decrease in fluorescence (excitation at 400 nm) and

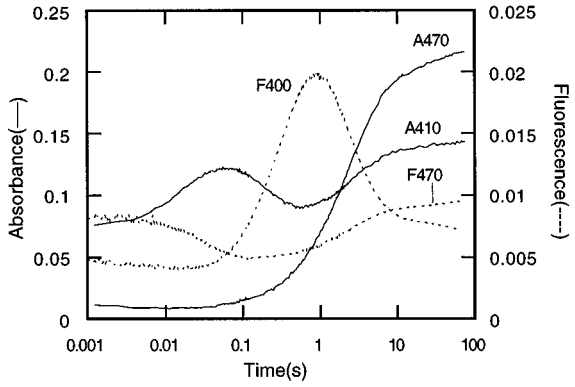

FIGURE 9: Kinetic traces from single wavelength measurements of the reoxidation of reduced enzyme−5HN complex in the presence of azide. The absorbance data from the experiment of Figure 8 displayed as single wavelength kinetics traces: (A410) data of 410 nm; (A470) data of 470 nm. In a separate experiment, the reaction of MHPCO−5HN complex (7.7 μM of enzyme and 200 μM 5HN) with 625 μM oxygen in the presence of 50 mM sodium azide was monitored in the fluorescence stopped-flow apparatus. Fluorescence data were recorded with excitation at 400 nm (F400) and at 470 nm (F470). Emission of light with wavelengths greater than 515 nm was detected. All experiments were performed in 95 mM sodium phosphate and 1 mM DTT, pH 7.0, 4 °C.

increase of fluorescence (excitation at 470 nm). This step is the conversion of the highly fluorescent intermediate, C(4a)-hydroxy-FAD species, to the oxidized enzyme. The existence of the slow fourth phase with a decrease of fluorescence (excitation at 400) and an increase of fluorescence (excitation at 470 nm) supported the existence of the intermediate III−5HN complex. The slow conversion of the intermediate III−5HN complex to the oxidized enzyme is demonstrated by the fluorescence decrease at 400 nm due to the intermediate and the fluorescence increase at 470 nm due to the oxidized enzyme during this fourth phase.

Scheme 5 describes the reoxidation of the E_{red}−5HN complex in the presence of azide. In this reaction scheme, oxygen reacts with the reduced enzyme−5HN complex to form the C(4a)-hydroperoxy-FAD enzyme (E_I−5HN). Oxygen transfer from the transient intermediate to 5HN yields the C(4a)-hydroxy-FAD−FAMS complex. FAMS then dissociates from the complex giving the C(4a)-hydroxy-FAD enzyme (E_{III}). A large fraction of this C(4a)-hydroxy-FAD enzyme rapidly converts to the oxidized enzyme species, but some of the C(4a)-hydroxy-FAD enzyme binds to the excess 5HN, resulting in the intermediate III−5HN complex. The reaction also includes 15% of an uncoupling pathway arising from the conversion of the C(4a)-hydroperoxy-FAD enzyme to the oxidized enzyme species. A similar sequence of reactions has been documented previously with phenol hydroxylase (Yorita & Massey, 1993)

Effect of 5HN concentration on the Kinetics of the Reoxidation of the Reduced Enzyme−5HN Complex in the Presence of Azide. To test whether the binding of 5HN to E_{III} can actually occur, the reduced enzyme−5HN complex was mixed with oxygenated buffer containing sodium azide and different concentrations of 5HN, and the reaction was monitored in the fluorescence stopped-flow instrument with excitation at 400 nm for detection of C(4a)-hydroxy-FAD species. The results are shown in Figure 10. The major effect of 5HN concentration is on the fluorescence accumulating at the beginning of the final phase. This result

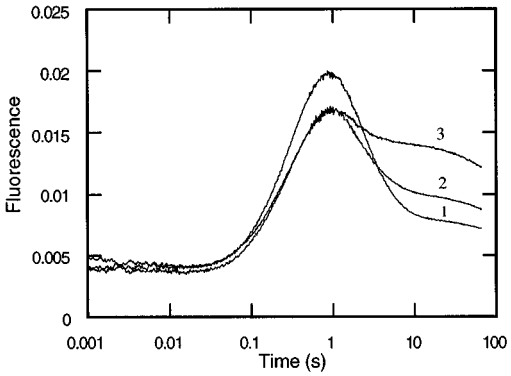

FIGURE 10: The reoxidation of reduced enzyme−5HN complex in equilibrium with different concentrations of 5HN. Reduced MHPCO (7.4 μM) was reacted with oxygen (625 μM) in the buffer solution containing 50 mM sodium azide and different concentrations of 5HN in the stopped-flow apparatus. The reaction was monitored by fluorescence with an excitation wavelength of 400 nm and emission of wavelengths greater than 515 nm. (1) 200 μM, (2) 400 μM, and (3) 800 μM of 5HN after mixing.

Scheme 6

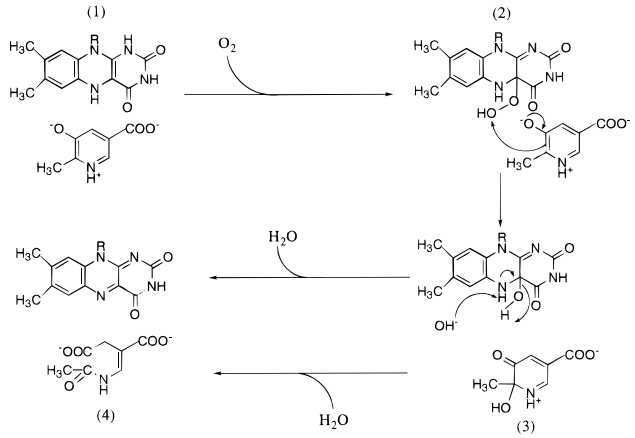

strongly suggests that this fluorescent intermediate is a mixture of oxidized enzyme and C(4a)-hydroxy-FAD enzyme−5HN complex as in Scheme 5. At higher concentrations of 5HN, greater fractions of the enzyme were trapped in the 5HN complex form, resulting in a higher level of fluorescence.

DISCUSSION

This work demonstrates that the oxidative half reaction of MHPCO involves the participation of two oxygenated flavin intermediates, the C(4a)-hydroperoxy flavin and the C(4a)-hydroxy flavin enzyme species, showing that the reaction mechanism bears strong resemblance to that of the flavoprotein hydroxylases.

On the basis of previous kinetic studies of aromatic flavoprotein hydroxylases (Ballou, 1984; Entsch et al., 1976; Schopfer & Massey, 1980; Detmer & Massey, 1985; Yorita & Massey, 1993; Powlowski et al., 1990), a tentative mechanism for the action of MHPCO is postulated in Scheme 6. In this mechanism, reaction of the reduced enzyme−substrate complex (species 1) with molecular oxygen produces the C(4a)-hydroperoxy flavin intermediate (species 2). Hydroxylation of the substrate involves nucleophilic displacement by the phenolate form of the substrate of the distal oxygen of the C(4a)-hydroperoxy flavin enzyme (step 2) yielding the C(4a)-hydroxy flavin enzyme and the hydroxy-

Scheme 7

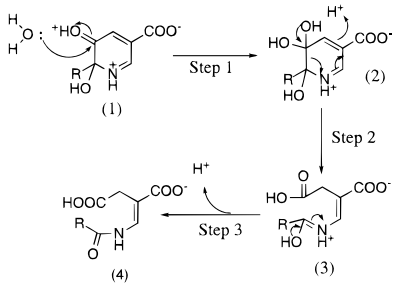

Scheme 8

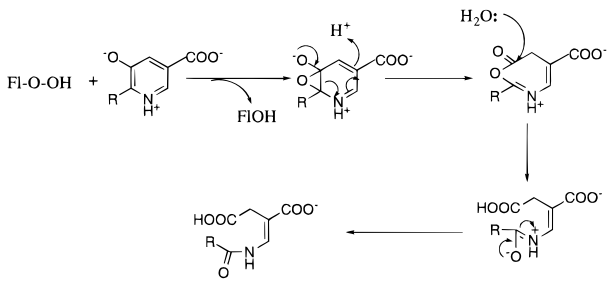

lated substrate species (species 3), analogous to the postulated cyclohexadienone substrate intermediate in the hydroxylation of *p*-hydroxybenzoate (Entsch et al., 1974) and the species postulated in phenol hydroxylase (Yorita & Massey, 1993). The flavin C(4a)-hydroxide intermediate decays to oxidized flavin enzyme and water while the hydroxylated MHPC undergoes a ring cleavage reaction to form AAMS.

Our data cannot exclude reversibility of steps in Scheme 6. However, there is considerable support that the steps are indeed all essentially irreversible. (a) In the reaction of E_{red} and O_2, an intercept of the plot of k_{obs} vs O_2 is near zero, indicating that the reaction is essentially irreversible. (b) Long-lived C(4a)-hydroxy flavins do not produce detectable C(4a)-hydroperoxy flavins. (c) E_{ox}, E_{ox}−substrate, or E_{ox}−product do not produce detectable C(4a)-hydroxy flavin. AAMS (or FAMS) does not produce the hydroxylated MHPC (or the hydroxylated 5HN) species. Thus, the K_{eq} for the forward reactions of Scheme 6 is very large and it is reasonable to describe our model as irreversible reactions.

This postulated hydroxylation mechanism is supported by oxygen-18 tracer experiments. Oxygen-18 labeling demonstrates that essentially one atom of oxygen from $^{18}O_2$ was incorporated in the product, AAMS. The incorporated label was located in the acetyl group of the product with only very little incorporation into the carboxymethyl moiety. This labeling pattern is consistent with single oxygen transfer from the C(4a)-hydroperoxide to MHPC as depicted in Scheme 6.

The ^{18}O labeling experiment in $H_2{}^{18}O$-enriched medium demonstrated that 0.59 atom of ^{18}O from $H_2{}^{18}O$ was incorporated in the carboxymethyl moiety, while only 0.15 atom was incorporated into the acetyl group of the product. This is consistent with the incorporation of one oxygen atom from H_2O to the carboxymethyl moiety. The poor recovery of label in the reaction mixture enriched with $H_2{}^{18}O$ may be due to loss of the label during preparation of the product for mass spectrometry.

These ^{18}O-labeling results are in agreement with previous oxygen-18 tracer experiments (Sparrow et al., 1969). Snell and co-workers (Sparrow et al., 1969) reported the incorporation of 0.95 and 0.14 atoms of oxygen from $^{18}O_2$ into the acetyl and carboxymethyl moieties of the product AAMS, respectively. In the reaction medium enriched with $H_2{}^{18}O$, they observed the incorporation of 0.38 atom of oxygen into the carboxymethyl group with little incorporation (0.07 atom) into the acetyl group of AAMS.

Formation of the product, AAMS, is thought to arise from hydration and ring cleavage of the transient hydroxylated MHPC species. Scheme 7 shows a possible mechanism for the hydration and ring scission reaction of the transient hydroxylated species. This postulated mechanism is consistent with the above ^{18}O-labeling results, demonstrating the incorporation of ^{18}O from $H_2{}^{18}O$ to the 3-position of the MHPC. When the enzymatic reaction was conducted in buffer solution prepared in D_2O, the product AAMS incorporated 1.0 atom of deuterium (Kishore & Snell, 1981). This observation is in agreement with the mechanism proposed, in which a proton (or deuteron) is taken up at the C(4) position of the product.

The hydroxylation and ring cleavage reaction of MHPC catalyzed by MHPCO is unusual among flavoprotein hydroxylases. For all known flavoprotein hydroxylases, the dienone intermediate [analogous to hydroxylated MHPC (species 1, Scheme 7)] is rearomatized to give the hydroxylated aromatic product (Massey & Hemmerich, 1975; Ballou, 1982; Palfey et al., 1996). However, the presence of a methyl group at the 2 position of the hydroxylated MHPC intermediate prevents such a rearomatization. It was of interest to find out whether cleavage of the dienone ring with MHPC was due to the inability of the substrate to rearomatize or due to the nature of the active site of the enzyme. The analysis of 5HN as a substrate could answer this question. If the enzyme were designed for simple hydroxylation, the product should be 5,6-dihydroxynicotinic acid (or its tautomer). However, since the product with 5HN was identified to be α-(*N*-formylaminomethylene)succinic acid (FAMS), it seems clear that the enzyme is designed for carrying out the cleavage in addition to the hydroxylation. This cleavage undoubtedly requires acidic and basic groups in the active site that are somewhat unique to flavoprotein hydroxylases.

An alternative mechanism for the oxygen atom transfer and the ring cleavage reaction, shown in Scheme 8, has been suggested by a reviewer. This involves the insertion of an oxygen atom from the flavin hydroperoxide to form a substrate epoxide. Since this mechanism involves the same flavin−oxygen intermediates as that of Scheme 7, our experimental data cannot distinguish these two mechanisms. However, the formation of the epoxide in Scheme 8, which involves the donation of an oxene equivalent from the flavin hydroperoxide, is unlikely to occur. (a) Bruice et al. (1983) have shown that C(4a)-hydroperoxy flavin model compounds do not react with 2,3-dimethyl-2-butene to form an epoxide product. 2,3-Dimethyl-2-butene would be more likely to form an epoxide compound than would MHPC. (b) Semiempirical orbital calculations (AM1 Hamiltonian) on epoxide species (Scheme 8) and species 1 in Scheme 7 suggest that the epoxide is about 25 kcal/mol less stable than species 1, Scheme 7.[2] Therefore, the mechanism shown in Scheme 7 is more plausible than that shown in Scheme 8 for the ring cleavage reaction.

[2] Palfey, B. A., unpublished result.

Another flavoprotein hydroxylase, anthranilate hydroxylase, also carries out an additional step after the hydroxylation. It hydrolyzes the 3-hydroxydienimine of anthranilate that forms in the hydroxylation reaction to effect the release of ammonia; this hydrolysis leads to a dienone species, which then rearomatizes to form the 2,3-dihydroxybenzoate product (Powlowski et al., 1987, 1990). Although it appears to be a dioxygenase reaction, the 2-hydroxyl of the product comes from water (Powlowski et al., 1987).

Data from our stopped-flow experiments indicate that the enzyme uses the same reaction pathway to catalyze both the MHPC and the 5HN reactions. The investigation of the reaction of the reduced enzyme−5HN complex with oxygen reveals the presence of the same transient intermediates as found in the reaction of the reduced enzyme−MHPC complex with oxygen, the C(4a)-hydroperoxy flavin and C(4a)-hydroxy flavin species. The rates of formation of intermediates in the 5HN reaction are comparable or slightly faster to those in the MHPC reaction. 5HN was shown to be as efficient a substrate as MHPC, since the hydroxylation stoichiometry with both reactions is greater than 90%.

In conclusion, MHPCO can be classified as a flavoprotein hydroxylase. Product analysis of the enzymatic reaction of 5HN and MHPCO demonstrates that this enzyme catalyzes both a classical hydroxylation and a subsequent unique hydrolysis of the hydroxylated substrate to yield the acyclic product.

ACKNOWLEDGMENT

We thank Dr. Scott Woehler for recording NMR spectra of the 5HN product. We thank Dr. Bruce A. Palfey for programming the Excel routine used to prepare data for global analysis and valuable discussions during the manuscript preparation.

REFERENCES

Arunachalam, U., & Massey, V. (1994) *J. Biol. Chem. 269*, 11795−11801.
Ball, S., & Bruice, T. C. (1980) *J. Am. Chem. Soc. 102*, 6498−6503.
Ballou, D. P. (1982) in *Flavins and Flavoproteins* (Massey, V., & Williams, C. H., Eds.) pp 301−310, Elsevier, Amsterdam.
Ballou, D. P. (1984) in *Flavins and Flavoproteins* (Bray, R. C., Engel, P. C., & Mayhew, S. G., Eds.) pp 605−618, Walter de Gruyter, Berlin, New York.
Balny, C., & Hastings, J. W. (1975) *Biochemistry 14*, 4719−4723.
Beaty, N. B., & Ballou, D. P. (1981) *J. Biol. Chem. 256*, 4619−4625.
Bruice, T. C., Noar, J. B., Ball S. S., & Venkataram, U. V. (1983) *J. Am. Chem. Soc. 105*, 2452−2463.
Bull, C., & Ballou, D. P. (1981) *J. Biol. Chem. 256*, 12673−12680.
Chaiyen, P., Brissette, P., Ballou, D. P., & Massey, V. (1997) *Biochemistry 36*, 2612−2621.
Dallacker, F., Fechter, P., & Mues, V. (1979) *Z. Naturforsch. B: Anorg. Chem., Org. Chem. 34*, 1729−1736.
Detmer, K., & Massey, V. (1984) *J. Biol. Chem. 259*, 11265−11272.
Detmer, K., & Massey, V. (1985) *J. Biol. Chem. 260*, 5998−6005.
Entsch, B., & Ballou, D. P. (1989) *Biochim. Biophys. Acta 999*, 313−322.
Entsch, B., Ballou, D. P., & Massey, V. (1974) *Biochem.Biophys. Res. Com. 57*, 1018−1025.
Entsch, B., Ballou, D. P., & Massey, V. (1976) *J. Biol. Chem. 251*, 2550−2563.
Ghisla, S., Entsch, B., Massey, V., & Husain, M. (1977) *Eur. J. Biochem. 76*, 139−148.
Hayaishi, O., Nozaki, M., & Abbott, M. J. (1975) in *The Enzymes*, 3rd ed. (Boyer, P. D., Ed.) Vol. 12, Part B, pp 119−189, Academic Press, New York.
Hitchman, M. L. (1978) in *Measurement of Dissolved Oxygen*, pp 21−29, John Wiley & Sons, New York.
Horecker, B. L., & Kornberg, A. (1948) *J. Biol. Chem. 175*, 385−390.
Howell, L. G., Spector, T., & Massey, V. (1972) *J. Biol. Chem. 247*, 4340−4350.
Husain, M., & Massey, V. (1979) *J. Biol. Chem. 254*, 6657−6666.
Kemal, C., & Bruice, T. C. (1976) *Proc. Natl. Acad. Sci. U.S.A. 73*, 995−999.
Kemal, C., Chan, T. W., & Bruice, T. C. (1977) *J. Am. Chem. Soc. 99*, 7272−7286.
Kishore, G. M., & Snell, E. E. (1979) *Biochem. Biophys. Res. Commun. 87*, 518−523.
Kishore, G. M., & Snell, E. E. (1981a) *J. Biol. Chem. 256*, 4228−4233.
Kishore, G. M., & Snell, E. E. (1981b) *J. Biol. Chem. 256*, 4234−4240.
Kishore, G. M., & Snell, E. E. (1981c) in *Oxygen and Oxy-Radicals in Chemistry and Biology* (Rodgers, M. A. J., & Powers, E. L., Eds.) pp 521−534, Academic Press, New York.
Levitt, M. J. (1973) *Anal. Chem. 45*, 618−620.
Massey, V., & Hemmerich, P. (1975) in *The Enzymes*, 3rd ed. (Boyer, P. D., Ed.) Vol. 12, Part B, pp 191−252, Academic Press, New York.
Nozaki, M. (1974) in *Molecular Mechanisms of Oxygen Activation* (Hayaishi, O., Ed.) pp 135−165, Academic Press, New York.
Palfey, B. A., Ballou, D. P., & Massey, V. (1996) in *Active Oxygen: Reactive Oxygen Species in Biochemistry* (Valentine, J. S., & Liebman, J. F., Eds.) pp 37−83, Chapman-Hall, New York.
Powlowski, J. B., Dagley, S., Massey, V., & Ballou, D. P. (1987) *J. Biol. Chem. 262*, 69−74.
Powlowski, J., Massey, V., & Ballou, D. P. (1989a) *J. Biol. Chem. 264*, 5606−5612.
Powlowski, J., Ballou, D. P., & Massey, V. (1989b) *J. Biol. Chem. 264*, 16008−16016.
Powlowski, J., Ballou, D. P., & Massey, V. (1990) *J. Biol. Chem. 265*, 4969−4975.
Schopfer, L. M., & Massey, V. (1980) *J. Biol. Chem. 255*, 5355−5363.
Strickland, S., & Massey, V. (1973) *J. Biol. Chem. 248*, 2953−2962.
Sparrow, L. G., Ho, P. K., Sundaram, T. K., Zach, D., Nyns, E. J., & Snell, E. E. (1969) *J. Biol. Chem. 244*, 2590−2600.
Tolman, V., & Sedmera, P. (1993) *Collect. Czech. Chem. Commun. 58*, 1430−1436.
Vervoort, J., Muller, F., Lee, J., van den Berg, W. A. M., & Moonen, C. T. W. (1986) *Biochemistry 25*, 8062−8067.
Wang, L.-H., & Tu, S.-C. (1984) *J. Biol. Chem. 259*, 10682−10688.
Wang, L.-H., Hamzah, R. Y., Yu, Y., & Tu, S.-C. (1987) *Biochemistry 26*, 1099−1104.
Williams, C. H., Jr., Arscott, L. D., Matthews, R. G., Thorpe, C., & Wilkinson, K. D. (1979) *Methods Enzymol. 62*, 185−198.
Yorita, K., & Massey, V. (1993) *J. Biol. Chem. 268*, 4134−4144.
Yu, Y., Wang, L.-H., & Tu, S.-C.(1987) *Biochemistry 26*, 1105−1110.

BI970089U